

FIG. 73. Variation in quadrupole splitting of the outer  $\text{Fe}^{2+}$  doublet (AA' in Fig. 69 right) as a function of the  $\text{Al}_2\text{O}_3 + \text{Fe}_2\text{O}_3$  contents of the calcic amphiboles of Bancroft & Brown (1975) [from Goldman (1979)].

peak assignment in the examination of as yet uncharacterized types of amphibole. As is apparent from the above discussion, the refinement and assignment of calcic amphibole spectra are not always straightforward; however, some of the problems can be circumvented by use of a combination of experimental techniques. Recent studies have shown the importance of temperature-dependent electron delocalization in

the analysis of Mössbauer spectra of minerals with mixed valence Fe in adjacent sites (Nolet & Burns 1979, Schwartz *et al.* 1980). This effect has not yet been documented in amphiboles but is of potential significance in mixed valence Fe-rich amphiboles, and could further complicate spectral interpretation.

#### INFRARED-ABSORPTION SPECTROSCOPY IN THE OH REGION

The fundamental band of the O-H stretching vibration is in the range  $1500\text{--}3800\text{ cm}^{-1}$ . The exact position of this band in the infrared region is a function of the strength of the hydrogen-oxygen bond; strong bonds are associated with higher frequencies, the lower end of the range being characteristic of symmetrical hydrogen bonds. In the spectra of amphiboles, the fundamental band occurs from  $3600\text{ to }3700\text{ cm}^{-1}$ , indicative of a strong hydroxyl bond and little or no hydrogen bonding; this is compatible with the O(3)-H distance of  $\sim 1.0\text{ \AA}$  found in crystallographic studies. End-member amphiboles show a single sharp stretching band for hydroxyl in this region. However, the principal stretching band in intermediate amphiboles shows considerable fine structure (Fig. 78) that has been attributed to cation substitution effects at those cation sites co-ordinated by the hydroxyl ion. This occurs as a result of the fact that the frequency of the stretching band varies with the actual cations bonded to the hydroxyl. Strens (1974) has shown in the talc structures that the frequency shift is a function of the electronegativity of the bonded cations. Figure 79 shows this also to be the case for the

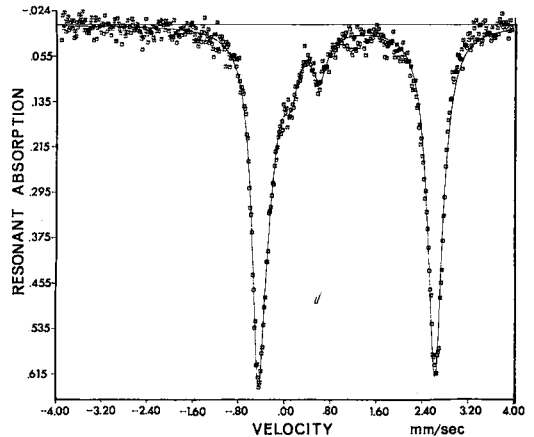
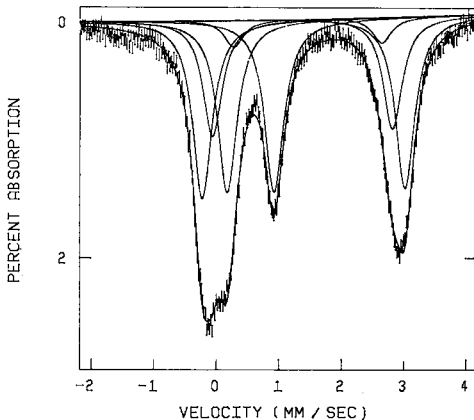


FIG. 74. Mössbauer spectra of richterite (right: liquid nitrogen temperature) and potassian ferri-taramite (left) [from Virgo (1972b) and Hawthorne (1973), respectively].

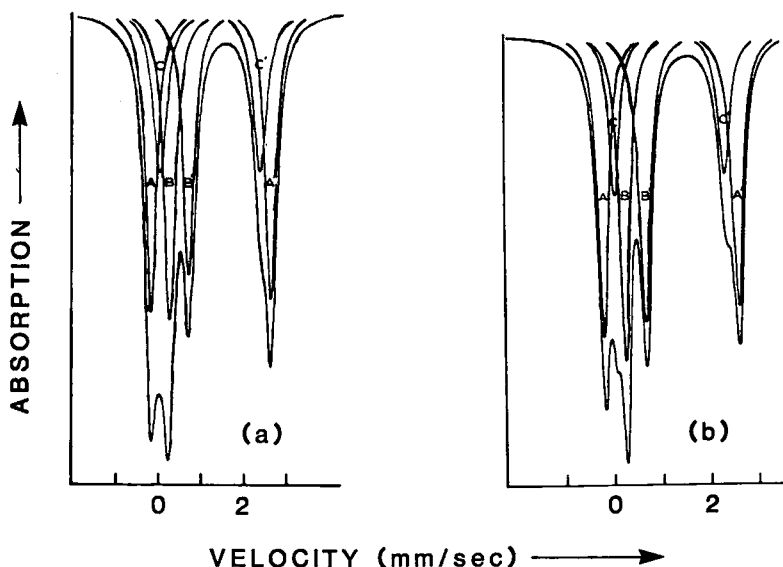


FIG. 75. Room-temperature Mössbauer spectra of crossite (left) and riebeckite (right) [from Bancroft & Burns (1969)].

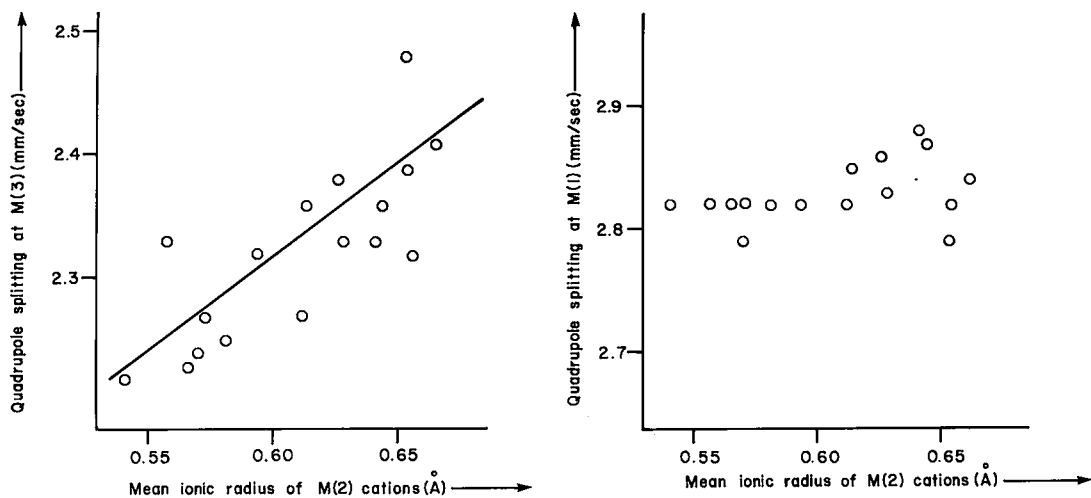


FIG. 76. Compositional systematics of the Mössbauer parameters in the alkali amphiboles. Data are taken from Appendix F.

amphiboles, and suggests that it is related to the relative covalency of the cation-hydroxyl bond, although undoubtedly many of the peaks are spurious and were assigned to configurations that produced agreement on plots such as these (*i.e.*, Fig. 79). In the amphibole structure, the OH group is bonded to two M(1) and one M(3) cations arranged in a pseudotrigonal manner around the O-H vector that is orthogonal to

the octahedral strip. Thus the relative intensities of the fine-structure bands contain significant information concerning the ordering of cations over the M(1) and M(3) sites.

Consider the case where the C-type cations are Mg and Fe<sup>2+</sup> only. There are eight possible ways of distributing two types of cations over the three M sites co-ordinating a single hydroxyl (Table 53). However, the three M sites co-

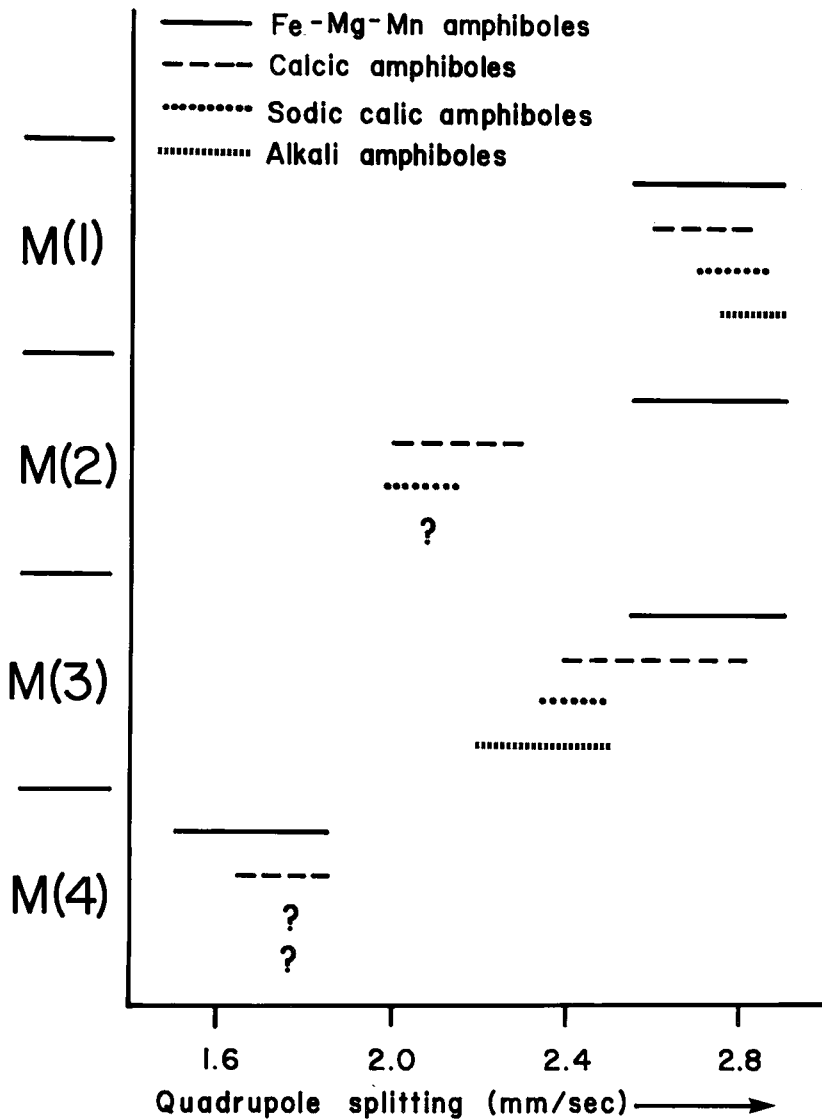


Fig. 77. Ranges of quadrupole splitting for  $\text{Fe}^{2+}$  at the M(1), M(2), M(3) and M(4) sites in amphiboles.

ordinating the hydroxyl are in a pseudotrigonal arrangement that introduces an accidental degeneracy to some bands and reduces the overall number of resolvable bands to four. Using the nomenclature of Table 54, the total  $\text{Fe}^{2+}$  content of the M(1) and M(3) sites in a binary ( $\text{Mg}, \text{Fe}^{2+}$ ) amphibole solid-solution is given by  $T = B_0 + 2C_0 + 3D_0$ .

If the total Fe content of the amphibole is known from the chemical analysis, the Fe content of the M(2) and M(4) sites may be

derived by difference. Where Mg and Fe are confined to the M(1) and M(3) sites, amphibole compositions may be derived. Strens (1966) proposed that the ratio  $\rho$  be used to indicate Mg-Fe ordering over the M(1) and M(3) sites, with  $\rho$  values greater than unity indicating preferential ordering of  $\text{Fe}^{2+}$  at the M(3) site.

Most amphiboles are considerably more complex than the above situation, and the presence of other cations at the M(1) and M(3) sites will give rise to additional bands. It is generally

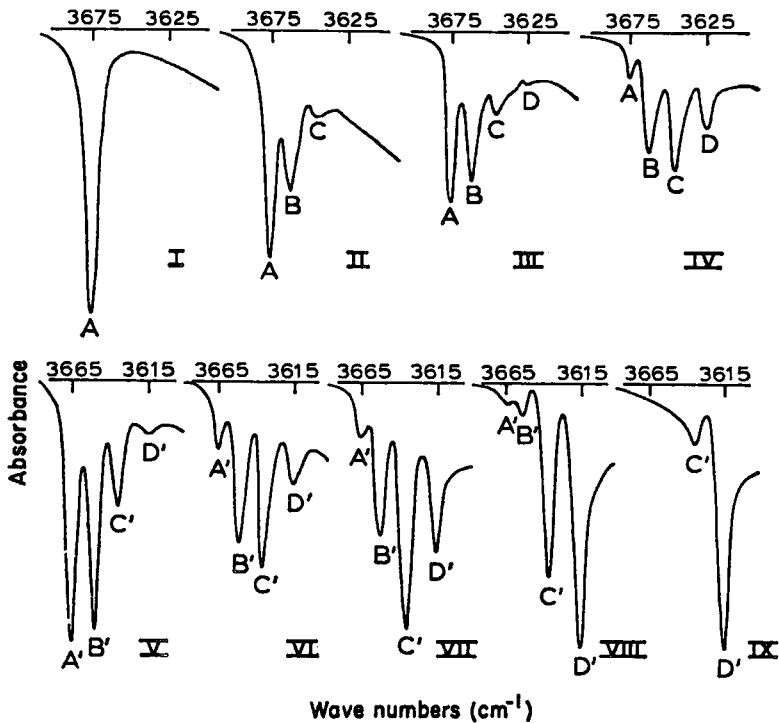


Fig. 78. Fine structure in the fundamental OH-stretching band in amphiboles of the magnesio-cummingtonite - grunerite series (lower) and the tremolite - ferro-actinolite series (upper) [from Burns & Strens (1966)]. The band nomenclature is given in Table 55. The compositions of the samples, expressed as  $\text{Fe}^{2+}/(\text{Mg} + \text{Fe}^{2+})$ , are as follows: I 0, II 0.15, III 0.30, IV 0.48, V 0.36, VI 0.53, VII 0.65, VIII 0.89, IX 0.98.

assumed that  $\text{Mn}^{2+}$  is indistinguishable in its effect from  $\text{Fe}^{2+}$ , but such cations as  $\text{Fe}^{3+}$ , Al, Li and Ti give rise to additional bands. Numerous subsidiary bands have been recognized in amphibole studies, and have generally been assigned to specific cation-configurations on the assumption that the frequency is a smooth function of some atomic parameter such as mass or electronegativity (Fig. 79). Table 55 is a compilation of the bands assigned in previous work; although many of these were assigned by mass or electronegativity arguments, the principal Mg-Fe bands were assigned from the results of heating experiments (see later section on oxidation studies).

Cation substitutions at other sites besides M(1) and M(3) can cause a frequency shift: (i) Each Ca present in the group of four M(4) positions around each A site increases the stretching frequency by  $\sim 2 \text{ cm}^{-1}$ . (ii) Alkali cations entering the A site increase the OH stretching frequency considerably [ $+24 \text{ cm}^{-1}$  in

riebeckite (Strens 1974),  $30\text{--}40 \text{ cm}^{-1}$ , for hastingsite and pargasite (Semet 1973),  $56 \text{ cm}^{-1}$  and  $62 \text{ cm}^{-1}$ , respectively, for richterite and potassium-richterite (Rowbotham & Farmer 1973)]. (iii) The substitution  $\text{Fe}^{3+} \rightleftharpoons \text{Al}$  at the M(2) site in alkali amphiboles (Bancroft & Burns 1969) appears to increase the stretching frequency slightly. Possibly substitution at the tetrahedral sites could also have a slight inductive effect in  ${}^{10}\text{Al}$  amphiboles. (iv) In orthorhombic amphiboles, the presence of two inequivalent hydroxyl groups results in a slight broadening of the band width to  $\sim 7 \text{ cm}^{-1}$  in anthophyllite (Burns & Law 1970).

In the more complex amphiboles, such as hornblende and gedrite, the large number of bands, together with the considerable broadening of bands, may result in spectra that are too complex to be resolved.

There are several problems associated with the application of this technique to general site-population studies. Problems associated with

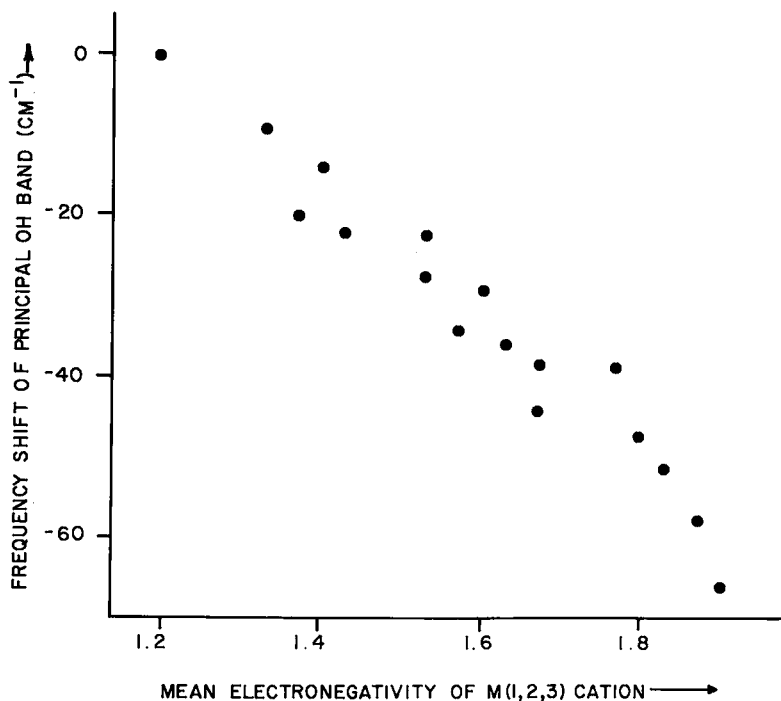


Fig. 79. Frequency shift of the principal OH band in  $C2/m$  amphiboles as a function of the mean electronegativity of the cations bonded to O(3).

TABLE 53. POSSIBLE CATION-ARRANGEMENTS AND HYDROXYL-STRETCHING BAND ASSIGNMENTS IN AMPHIBOLES WITH M(1,2,3) COMPLETELY OCCUPIED BY Mg AND Fe<sup>2+</sup>

M(1)	M(2)	M(3)	M(1)≠M(3) <sup>1</sup>	M(1)~M(3) <sup>2</sup>
Mg	Mg	Mg	A	A
Mg	Mg	Fe <sup>2+</sup>	B'	B
Mg	Fe <sup>2+</sup>	Mg	B''	B
Fe <sup>2+</sup>	Mg	Mg	B'''	B
Fe <sup>2+</sup>	Fe <sup>2+</sup>	Mg	C'	C
Fe <sup>2+</sup>	Mg	Fe <sup>2+</sup>	C''	C
Mg	Fe <sup>2+</sup>	Fe <sup>2+</sup>	C'''	C
Fe <sup>2+</sup>	Fe <sup>2+</sup>	Fe <sup>2+</sup>	D	D

TABLE 54. NOMENCLATURE OF LAW (1976) USED IN THE DISCUSSION OF CATION ORDERING AND BAND INTENSITIES IN INFRARED SPECTRA

$T_f$	total Fe <sup>2+</sup> at M(1) and M(3) sites
$\mu_I, \phi_I$	site-occupancies of Mg and Fe <sup>2+</sup> at M(I)
$A_o$	normalized observed intensity of peak A
$A_r$	value of intensity of peak A for random distribution
$A_c$	calculated value of intensity of peak A
$e$	$(B_o/B_r)/(C_o/C_r)$
$e_c$	$(B_c/B_r)/(C_c/C_r)$

<sup>1</sup>ideal band-assignment for crystallographically distinct configurations

<sup>2</sup>band assignments for configurations with accidental degeneracy due to pseudo-trigonal arrangement

the curve-fitting procedure are discussed by Hawthorne (1983). One important point has been raised by Strens (1974). In principle, vibrational bands are Lorentzian in form, but Strens (1974) has claimed that line broadening usually results in a band shape that approximates

a skewed Gaussian function. If this is the case, use of normal Gaussian curve-shape in the spectrum refinement will give rise to spurious bands. Many of the minor bands in previous studies could be of this origin.

The derivation of ordering patterns from band intensities assumes that the band intensity for a specific configuration is related to the frequency of occurrence of that configuration in the same way as all other bands are related to their corresponding configurations. Thus the transition moment of the OH stretch is assumed to be independent of the type of

TABLE 55. FREQUENCY SHIFT OF PRINCIPAL OH BAND RELATIVE TO THE A BAND FOR VARIOUS CATION CONFIGURATIONS<sup>1</sup>

Band	Configuration	Displacement (cm <sup>-1</sup> )
A	MgMgMg	0
B	MgMgFe <sup>2+</sup>	-14
C	MgFe <sup>2+</sup> Fe <sup>2+</sup>	-29
D	Fe <sup>2+</sup> Fe <sup>2+</sup> Fe <sup>2+</sup>	-47
E	MgMgFe <sup>3+</sup>	-22
F	MgFe <sup>2+</sup> Fe <sup>3+</sup>	-36
G	MgFe <sup>3+</sup> Fe <sup>3+</sup>	-44
H	Fe <sup>2+</sup> Fe <sup>2+</sup> Fe <sup>3+</sup>	-51
I	Fe <sup>2+</sup> Fe <sup>3+</sup> Fe <sup>3+</sup>	-58
J	Fe <sup>3+</sup> Fe <sup>3+</sup> Fe <sup>3+</sup>	-66
K	MgMgAl	-9
L	MgFe <sup>2+</sup> Al	-22
M	Fe <sup>2+</sup> Fe <sup>2+</sup> Al	-38
N	MgAlAl	-
O	Fe <sup>2+</sup> AlAl	-38
P	MgFe <sup>3+</sup> Al	-
Q	Fe <sup>2+</sup> Fe <sup>3+</sup> Al	-
-	LiFe <sup>2+</sup> Fe <sup>2+</sup>	-27
-	LiFe <sup>2+</sup> Fe <sup>3+</sup>	-34
-	LiMgFe <sup>3+</sup>	-20
-	Na at A	+24
-	K at A	+31
-	Al for Si	-75
-	Ti at M(1,2,3)	-87, -99
-	Ca at M(4)	+2n, 0 < n < 4

<sup>1</sup> data taken mainly from Strens (1974) and Bancroft & Burns (1969): band nomenclature slightly modified. Configurations R, S and T of Bancroft & Burns (1969) not included. Bands E-Q should not be considered as definitely established. Each specific band configuration is permutable

configuration. Work on micas (Rouxhet 1970) suggests that this is not the case; however, there

is no evidence either way for the amphiboles. The occurrence of weak hydrogen bonding may significantly affect the transition moment of the OH band, whether or not the strength of the hydrogen bonding is related to the cation configuration at the co-ordinating octahedral sites.

Band-intensity considerations have been used to derive site occupancies in a variety of amphiboles. A general survey is given here, and detailed quantitative results are given in Appendix G.

#### Fe-Mg-Mn amphiboles

Spectra for the orthorhombic amphiboles anthophyllite and gedrite are reported by Strens (1966), Bancroft *et al.* (1966) and Burns & Law (1970). A typical spectrum (Fig. 80) shows four bands (A-D) that can be assigned to the various possible Mg/Fe configurations (Table 53), together with minor peaks that were assigned to configurations involving Al. The peak half-widths of the anthophyllite (and gedrite) spectra are significantly wider than in the corresponding monoclinic Fe-Mg-Mn amphiboles (Fig. 78). Burns & Law (1970) ascribed this to the fact that the *Pnma* amphibole structure has two crystallographically distinct OH positions. The environment of each position is slightly different, thus leading to slight differences in the stretching frequency sufficient to broaden each peak but not to split it into two resolvable components; Burns & Law (1970) referred to this as "chain broadening". Inspection of Figure 80 also shows that the peaks B and C are significantly wider than peaks A and D. Peaks B and C are each composed of pseudo-symmetrically degenerate components (see Table 53); breakdown of the trigonal pseudo-symmetry results in only incomplete overlap of the individual components and a broadening of the composite peaks. The A and D peaks result from configurations involving only one cation and thus are not susceptible to this effect; hence the A and D bands are narrower than the B and C bands. Burns & Law (1970) called this "permutation broadening". The deviation of the experimental points and calculated curve to the high-frequency side of the A band may be due to an additional band at  $\sim 3667$  cm<sup>-1</sup> that can be associated with local A-site occupancy by Na (*cf.* richterite spectra of Rowbotham & Farmer 1973). The holmquistite spectrum (Wilkins *et al.* 1970, Law & Whittaker 1981) is very similar to that of the other Fe-Mg-Mn amphiboles (Fig. 81),

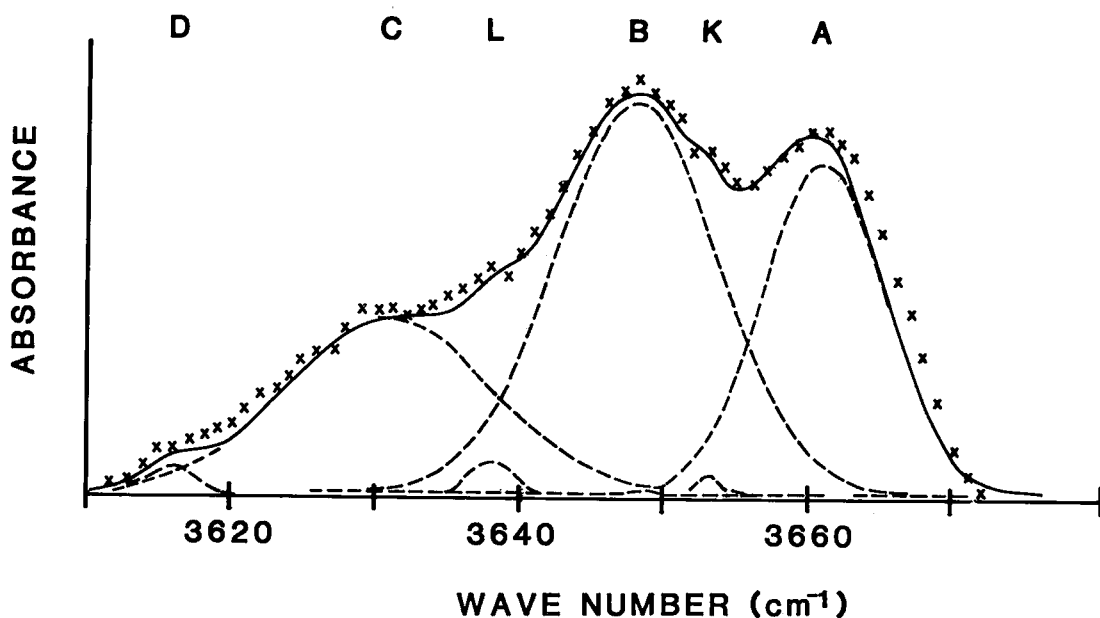


FIG. 80. Infrared absorption spectrum of anthophyllite in the hydroxyl-stretching region [from Burns & Law (1970)]. Band nomenclature as in Table 55.

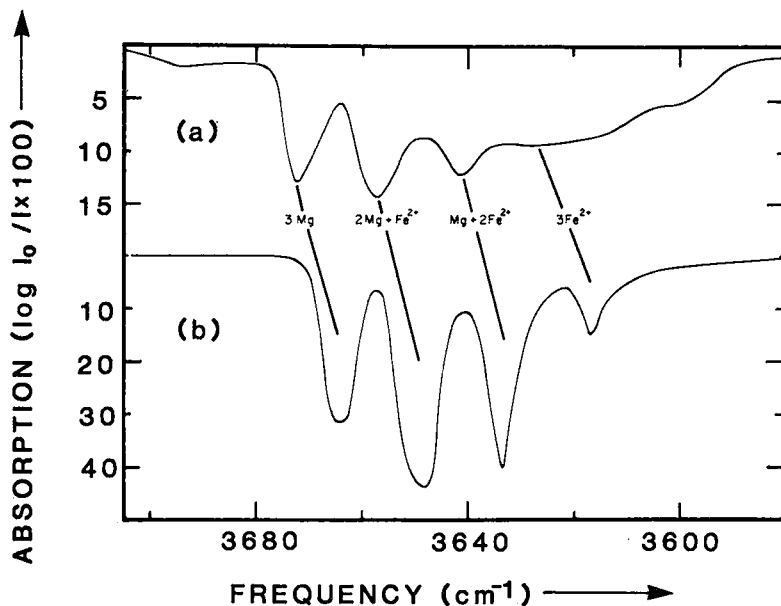


FIG. 81. Infrared absorption spectrum of holmquistite (top) and magnesiohornblende (bottom) [from Wilkins *et al.* (1971)].

as the occupancy of the M1 and M3 sites is very similar throughout this group.

Following the experimental results of Fabries & Perseil (1971), Law (1981) has shown that

the principal fine-structure bands in anthophyllite are split into hyperfine components. There are four components of the A band, and the intensity of the highest-frequency absorption

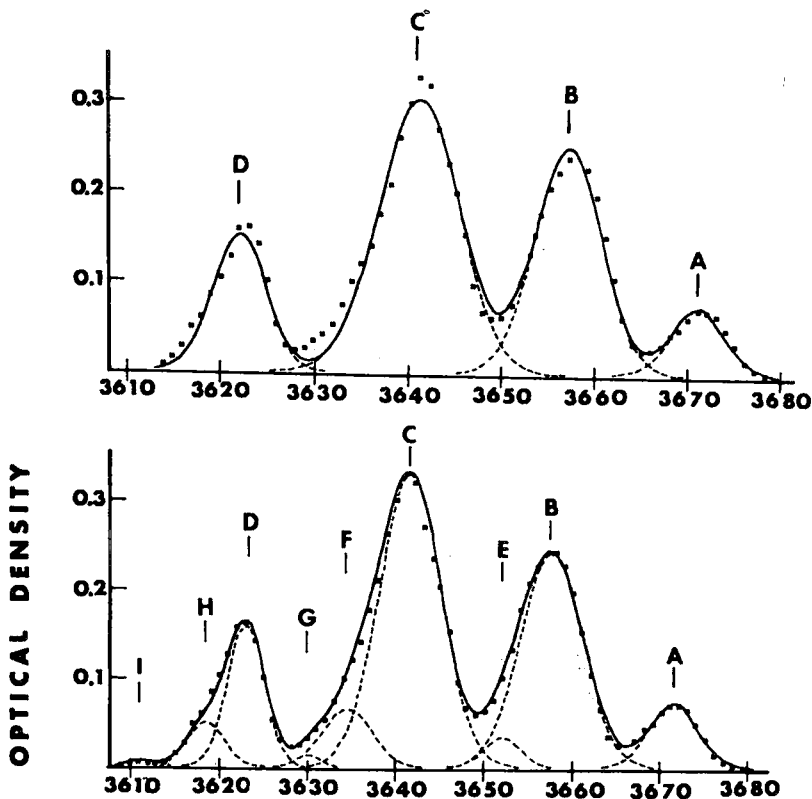


FIG. 82. Replotted infrared absorption spectrum (OH region) of manganous ferro-actinolite showing the existence of minor bands when fitting normal gaussian peak shapes. Top: 4-peak fit, bottom: 9-peak fit [from Burns & Greaves (1971)]. Band nomenclature as in Table 55.

decreases with increasing Al and  $\text{Fe}^{3+}$  in the amphibole. The origin of these bands is not clear.

Spectra for the amphiboles of the magnesio-cummingtonite-grunerite series have been reported by Strens (1966), Burns & Strens (1966) and Buckley & Wilkins (1971); spectra for several amphiboles of this series are shown in Figure 78. These are simple four-peak spectra that may be assigned as in Table 53.

#### Calcic amphiboles

Tremolite - ferro-actinolite spectra are reported by Burns & Strens (1966), Strens (1966), Wilkins (1970) and Burns & Greaves (1971); a typical series of spectra is shown in Figure 78. The four prominent bands are associated with the configurations of Table 53. However, attempts to fit the spectra to symmetrical Gaussian peaks (in order to derive site occupancies) lead to a poor fit on the low-frequency

side of each peak; these discrepancies have been ascribed to occupancy of M(1) and M(3) by other cations (e.g.,  $\text{Fe}^{3+}$ , Al, Li) in addition to Mg and  $\text{Fe}^{2+}$ , and minor peaks have been fitted to the spectra (Fig. 82). It is possible (Strens 1974) that many of these minor peaks are spurious, and that the correct line-shape is a skewed Gaussian and not a symmetrical Gaussian function.

A magnesio-hornblende spectrum (Fig. 81) was reported by Wilkins *et al.* (1970); the four principal bands due to Mg- $\text{Fe}^{2+}$  are prominent, but they are broad, and additional ill-defined absorption occurs. This is probably "substitutional broadening" as described by Robbins & Strens (1972) in the micas. Semet (1973) reported spectra for the synthetic amphiboles magnesio-hastingsite and pargasite (Fig. 83). The magnesio-hastingsite has variable  $\text{Fe}^{3+}/\text{Fe}^{2+}$  ratios depending on the  $f(\text{O}_2)$  conditions of synthesis, and thus bands due to configurations involving  $\text{Fe}^{2+}$  are present (3675 and 3642



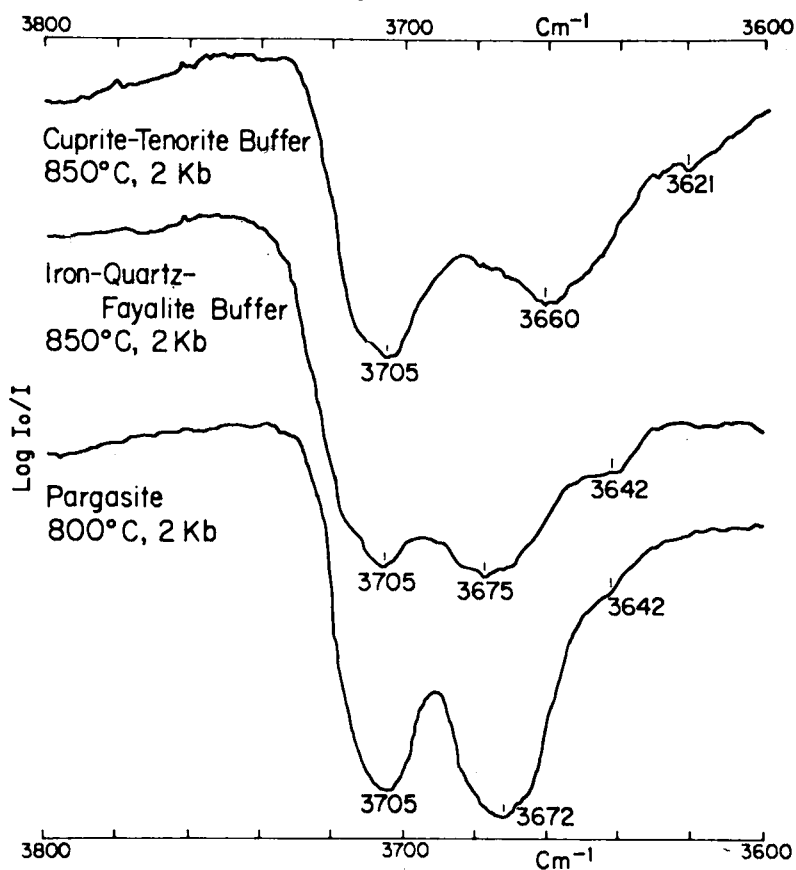


FIG. 83. Infrared absorption spectra of magnesio-hastingsite crystallized at different buffers (top two spectra) and pargasite (bottom spectrum) [from Semet 1973].

$\text{cm}^{-1}$ ); on the cuprite-tenorite buffer, where Mössbauer spectra showed no  $\text{Fe}^{2+}$  in the amphibole product, the 3660 and 3621  $\text{cm}^{-1}$  bands must be due to configurations involving  $\text{Fe}^{3+}$ . Similarly for the pargasite spectrum, the 3672 and 3642  $\text{cm}^{-1}$  bands presumably involve configurations with Al at M(1) or M(3) (or both); in fact, derivation of the band intensities (Semet 1973) indicates that Al is distributed randomly over the M(1), M(2) and M(3) sites in this synthetic pargasite.

#### Sodic-calcic amphiboles

Spectra for synthetic richterite and potassium-richterite were presented by Rowbotham & Farmer (1973) and are shown in Figure 84, together with a spectrum of an amphibole intermediate between richterite and tremolite. The effect of the A-site cation is to shift the

peak (assignable to an  $\text{MgMgMg-OH}$  configuration) to higher frequencies. However, each richterite shows the presence of a tremolite-type peak, suggesting that the amphibole is not pure end-member richterite; the fact that this is more prominent for richterite than for potassium-richterite suggests that this may be due to Na loss during preparation or synthesis of the amphibole.

#### Alkali amphiboles

Alkali amphibole spectra have been reported by Strens (1966, 1974), Burns & Prentice (1968), Bancroft & Burns (1969) and Ernst & Wai (1970); typical spectra are shown in Figure 85. Consider first the spectra of the glaucophane and cossite specimens. Bancroft & Burns (1969) resolved the spectra into the four major A-D bands, together with minor

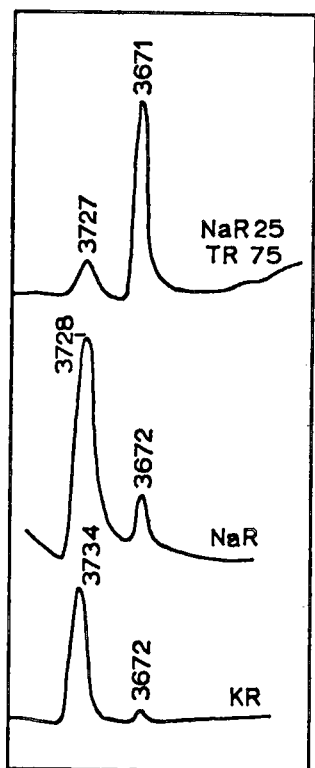


FIG. 84. Infrared absorption spectra of a solid solution of 75% tremolite and 25% richterite (top), richterite (middle) and potassium richterite (bottom) [from Rowbotham & Farmer (1973)]. Note the weak peaks at the tremolite position in richterite.

bands involving Al and  $\text{Fe}^{3+}$  at M(1) or M(3) (or both). Strens (1974) resolved the spectra into four bands only, each of which exhibited a skewed Gaussian line-shape and substitutional broadening that varied from sample to sample; Strens (1974) suggested that the minor peaks found in earlier studies were primarily artifacts of the fitting procedure when using symmetrical Gaussian line-shapes. Burns & Prentice (1968) and Strens (1974) studied the same three amphiboles (crocidolite) from the magnesio-riebeckite-riebeckite series (Fig. 85); again, the earlier study assigned several minor bands that were not found in the later work. However, some minor bands were recognized in these metamorphic amphiboles by Strens (1974); the  $A^1$  band is the A band shifted to higher frequencies by the presence of A-site Na (*cf.* Fig. 84), whereas the F and H bands involve configurations with  $\text{Fe}^{3+}$  at M(1) or M(3). Detailed

crystal-structure refinements of metamorphic amphiboles of the glaucophane-ferro-glaucophane-magnesio-riebeckite-riebeckite series (Ungaretti *et al.* 1978) show no Al or  $\text{Fe}^{3+}$  at M(1) or M(3), supporting the contention of Strens (1974) that most of the assignments of minor bands in the earlier studies are false. In addition, Ungaretti (1980) has shown that oxidation of  $\text{Fe}^{2+} \rightarrow \text{Fe}^{3+}$  is accompanied by migration of Na from the M(4) site into the A site; thus sample oxidation would be expected to give rise to bands involving  $\text{Fe}^{3+}$  together with an  $A^1$  band indicating movement of Na from M(4) to A ( $B^1$ ,  $C^1$  and  $D^1$  are presumably also present but buried beneath the main part of the spectrum).

The spectrum of igneous riebeckite is quite different (Fig. 85). There is a very prominent D band showing considerable substitutional broadening ( $\sim 10 \text{ cm}^{-1}$  width instead of  $\sim 5 \text{ cm}^{-1}$  for the metamorphic blue amphiboles), a weak C band and no A or B bands, as expected for amphiboles with very little Mg. However, there are numerous minor bands; these are due to substitutions that are typical of igneous riebeckite but insignificant or absent in metamorphic riebeckite. Thus,  $\text{LiFe}^{2+}_2$  gives rise to a band at  $\sim D+20 \text{ cm}^{-1}$  (Addison & White 1968b), and the presence of A-site Na, Ca at M(4), Al at T(1) and F at O(3) will produce shifted D bands. Thus samples of igneous riebeckite have quite complex spectra.

#### General considerations

There are several factors that suggest that this method is not generally suitable for highly accurate site-occupancy studies in amphiboles, although it can be extremely useful in certain instances. The O(3) position may be occupied by F,  $\text{O}^{2-}$  and Cl in addition to OH. Thus in order to derive site occupancies in OH-deficient amphiboles, it is necessary to assume random mixing of the O(3) anions with no segregation at specific M(1)M(1)M(3) cation configurations. Unfortunately, the latter would not appear to be the case, either in F-rich amphiboles where  $\text{Fe}^{2+}$  tends to avoid F-co-ordinated sites (Cameron 1970, Rosenberg & Foit 1977), or in oxy-amphiboles where higher-valence cations ( $\text{Fe}^{3+}$ , Ti) are closely associated with  $\text{O}^{2-}$  at the O(3) position (Kitamura *et al.* 1975).

The criterion for ordering discussed above is rather misleading. This is quite a subtle argument, the details of which are given by Law (1976). Consider the standard equations relating peak intensity to mole fraction:

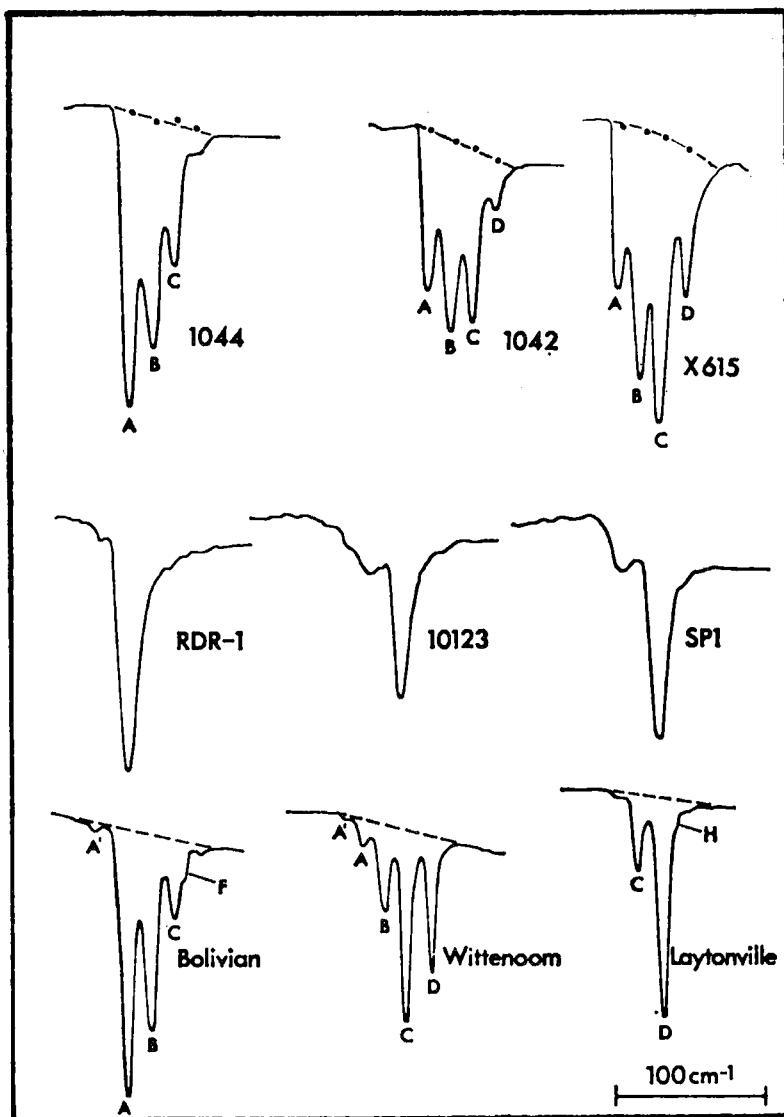


FIG. 85. Infrared absorption spectra of alkali amphiboles. Top: three samples of glaucophane showing typical four-band spectrum. Middle: three samples of riebeckite showing very prominent substitutionally broadened D bands and many minor bands. Bottom: three samples of metamorphic magnesio-riebeckite (crocidolite) showing well-resolved narrow four-band spectrum with additional minor bands A' (A shifted by Na at A site) and H [from Strens (1974)].

$$A_c = \mu_1^2 \mu_3 = (1-\phi_1)^2 (1-\phi_3)$$

$$B_c = \mu_1^2 \phi_3 + 2\mu_1 \phi_1 \mu_3 \\ = (1-\phi_1)^2 \phi_3 + 2(1-\phi_1)\phi_1(1-\phi_3)$$

$$C_c = \phi_1^2 \mu_3 + 2\mu_1 \phi_1 \mu_3 \\ = \phi_1^2 (1-\phi_3) + 2(1-\phi_1)\phi_1 \phi_3$$

$$D_c = \phi_1^2 \phi_3 = \phi_1^2 \phi_3$$

As  $\phi_1 = \frac{1}{2}(T_r - \phi_3)$ , each of the peak inten-

sities can be related to the single variable  $\phi_3$ . The behavior of  $A_c$ ,  $B_c$ ,  $C_c$ ,  $D_c$ , and  $\rho_c$  with varying  $\phi_3$  is strongly a function of  $T_r$  (that is, the chemical composition of the amphibole). This can be seen in Figure 86, which shows the behavior of these parameters as a function of  $\phi_3$  (the site-occupancy variable) for amphi-

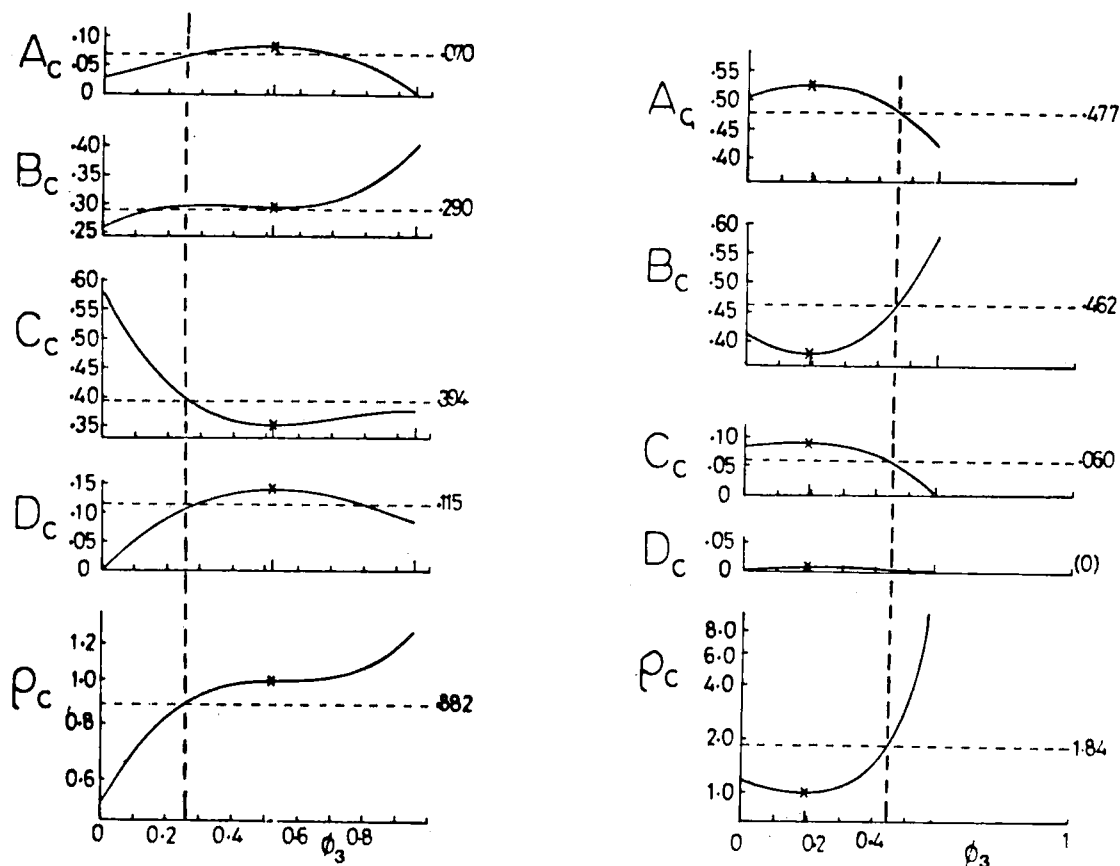


FIG. 86. Variation of calculated band-intensities as a function of  $M(3)$  site-population  $\phi_3$  for two samples of actinolite; observed band-intensities are indicated by the horizontal broken lines, and the solution for  $\phi_3$  is indicated by the vertical broken lines [modified from Law (1976)].

boles of different bulk-composition. Site occupancies may be derived by setting  $A_c \dots$  equal to  $A_o \dots$  in the above equations and solving for  $\phi_3$ ; four values of  $\phi_3$  are obtained, and hence where the solution is poorly defined by one or more equations, a fairly precise value is still obtainable from the remaining equations.

Inspection of Table 53 shows that the B and C bands are composed of nearly degenerate components  $B'$ ,  $B''$  and  $C'$ ,  $C''$ ; Strens (1974) suggested that  $B'/B''$  and  $C'/C''$  provide a sensitive measure of the degree of order, provided adequate resolution of the closely overlapping bands can be obtained. Problems involved in this procedure will be similar to those involved in the fitting of Mössbauer spectra, and hence similar techniques are required; Strens (1974) recommended the use of half-width constraints on  $B'$ ,  $B''$  and  $C'$ ,  $C''$  peaks. The method of Law (1976) appears much simpler to use.

Clustering is the tendency for the arrangements  $[\text{FeFeFe}]-\text{OH}$  and  $[\text{MgMgMg}]-\text{OH}$  to occur more often than expected for random mixing. Strens (1966) noted that the infrared absorption technique is sensitive to this effect, and suggested that clustering is indicated if the observed intensities of the A and D bands ( $A_o$  and  $D_o$ ) exceed the calculated values assuming random mixing. Law (1976) questioned the validity of this criterion for ordering, and Whittaker (1979) has systematically examined the behavior of band intensities with variation in degree of clustering and anticlustering (the mutual avoidance of like cations). Clustering of Fe increases the intensity of both the A and D bands (although not equally) and anticlustering of Fe has the reverse effect. However, the intensities of the B and C bands are also affected by clustering in a very complex manner that is also a function of bulk composition. If

clustering proves to be a common effect in amphiboles, it will almost certainly preclude any widespread use of the infrared absorption method in cation-ordering studies.

#### ELECTRONIC ABSORPTION SPECTROSCOPY OF AMPHIBOLES

When light passes through a crystal containing a transition-metal ion, certain wavelengths are absorbed by excitation of electrons between the nondegenerate  $3d$ -orbital energy-levels. As the character and amount of separation of the orbital energy-levels are a function of the potential field applied by the crystal, occupancy of the different sites in a crystal will produce absorption of different wavelengths of light. Hence, electronic absorption spectra can be used to characterize site occupancy in crystals both qualitatively (by observation and assignment of spectral bands to specific cations in specific sites: Burns 1970a) and quantitatively (by comparison of intensities of spectral bands: Burns 1970b). This method is not straightforward; the interpretation of the spectra is not easy, as illustrated by the work on the orthopyroxenes (White & Keester 1966, 1967, Bancroft & Burns 1967, Burns 1969, Runciman *et al.* 1973, Goldman & Rossman 1976, 1977b). The spectra may also be complicated by inter-element electron-transitions (Burns 1981), *i.e.*, intervalence charge-transfer bands (IVCT), where transitions are from cation to anion, anion to cation or cation to cation. These transitions are particularly common where adjacent cations have variable valence states (*e.g.*,  $\text{Fe}^{2+}$  and  $\text{Fe}^{3+}$ ,  $\text{Ti}^{3+}$  and  $\text{Ti}^{4+}$ ,  $\text{Fe}^{2+}$  and  $\text{Ti}^{4+}$ ) and are a major cause of color and pleochroism in amphiboles (Manning & Nickel 1969, Faye & Nickel 1970, Strens 1970). The intensity of this type of band is about two orders of magnitude larger than the intensity of normal  $d-d$  transitions. Thus overlap of these two types of band in an absorption spectrum can obscure the  $d-d$  transition bands. The occurrence of more than one type of transition-metal cation in the structure, as is common in most amphiboles, will further complicate the interpretation of the absorption spectra. For the derivation of quantitative site-occupancies, additional problems arise. The intensity of an absorption is a function of the probability of occurrence of the transition. The transition probability is governed by the Laporte selection rule (King 1964), which forbids transitions between  $3d$  orbitals. When a transition-metal cation occupies a site without a centre of

symmetry, mixing of the  $3d$  and  $4p$  orbitals allows a transition, the intensity of which is a function of the degree of  $3d-4p$  mixing that is, in turn, related to the deviation of the cation environment from centrosymmetry. Thus when a transition-metal cation occurs in more than one site in a crystal, the intensities of the  $d-d$  bands are a function of both the cation occupancies and the deviation of the cation environment from centrosymmetry. In centrosymmetric sites, some  $3d-4p$  orbital mixing may occur by vibronic coupling, and hence very weak bands can result from cations in these sites. Local disorder can also give rise to intensification of  $d-d$  bands in solid solutions; Robbins & Strens (1972) have noted this effect in micas and termed it "substitutional intensification". This could lead to nonlinear relationships in Beer's-law-type plots. These arguments suggest that calibration may be a problem for quantitative site-occupancy derivation. Conversely, this technique potentially has a qualitative sensitivity that the other common techniques lack.

Early work on amphiboles include that of Melankholin (1956), Chesnokov (1961), Littler & Williams (1965) and White & Keester (1966); these studies illustrated the importance of charge transfer on the pleochroism of amphiboles but encountered difficulties in the assignment of  $d-d$  bands. The last decade has seen great improvements in instrumentation, experimental technique and interpretation; this has been greatly aided by our increased understanding of the crystal chemistry of amphiboles and the co-operative use of other techniques; a general survey of the results follows.

#### *Fe-Mg-Mn amphiboles*

Mao & Siefert (1974) reported the polarized electronic absorption spectra of anthophyllite and gedrite (these are, respectively, anthophyllite[23] and gedrite[32] of Appendix C); the spectra are shown in Figure 87. The anthophyllite spectra are dominated by an intense band at  $\sim 10800\text{ cm}^{-1}$  that is particularly intense in the  $\beta$  spectrum and a broad intense band at  $\sim 4200\text{ cm}^{-1}$  that is particularly intense in the  $\alpha$  spectrum. These are assigned to  $d-d$  transitions in  $\text{Fe}^{2+}$  at the M4 site; the predominance of these bands is a result of the very noncentrosymmetric configuration of the environment about the M4 site that allows violation of the Laporte selection rule. The polarization characteristics of these bands are also compatible with this assignment. The remaining features of the spectra are much less intense. The sharp spike in the  $\alpha$  spectrum at